ACS OMEGA

Open Access

http://pubs.acs.org/journal/acsodf

Article

Experimental Study on the Effects of Washing Time, Washing Temperature, and Particle Size on the Combustion and Ash Formation Characteristics of Rice Husk

Shuo Yang,* Jintao Luo, Yu Gao, Shaohui Wang, Yupeng Zhang, Yuhang Wang, Pushi Ge, Wanqi Li, Yunyi Zheng, Jie Cui, Yudong Fu, and Honggang Pan

Cite This: *ACS Omega* 2024, 9, 50705−50719

Read Online

ACCESS | Metrics & More | Article Recommendations

ABSTRACT: There are many problems in the direct combustion of biomass, such as low combustion efficiency and easy slagging. In this paper, rice husk (RH) was taken as the research object, and the effects of different washing pretreatment conditions (washing time (WTI), washing temperature (WTE), and particle size) on the combustion characteristics and ash formation characteristics were discussed. The results show that the combustion characteristics of RH were significantly coupling-affected by the WTE and WTI, and the comprehensive characteristics of volatile release were significantly coupling-affected by the particle size and WTI. Specifically, under the condition of high-temperature washing, prolonging the WTI will increase the ignition temperature of washed RH powder. The particle size could affect the temperature of the maximum rate of decomposition. Under the same conditions, the temperature difference of maximum rate of decomposition between washed RH powder and RH was 5−10 °C. For the original RH, the longer the WTI, the more unfavorable it was to increase the maximum weight loss rate, and the opposite was true for RH powder. With the increase in WTE, the flammability index, burnout temperature, and volatile devolatilization initial temperature increased obviously. In addition, washing pretreatment could reduce the ashing quality of RH and RH powder to varying degrees, and the ash quality was decreased by about 15% compared with that of unwashed RH. The alkali metal removal effect of washed RH powder was better than that of washed RH. The proportion of alkali metal K was decreased from 1 to 4% (washed RH) to 0.2−1% (washed RH powder). The ash deposit and slagging phenomenon were obviously improved. Under the same WTI, the higher the WTE was, the better the removal effect of alkali metals was. Correspondingly, the proportion of the eutectic composite salt of Mg−Fe−Al with a high melting point increased in the high-temperature sintering stage, which effectively improved the ash melting point and reduced the probability of ash deposit and slagging.

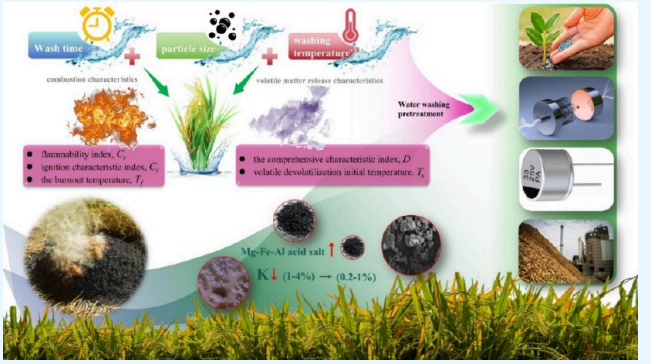

1. INTRODUCTION

Northeast China, as one of the main rice-producing areas, has extremely rich rice husk resources. According to the rice production data in Northeast China published by the National Bureau of Statistics of China in 2023, the annual output of rice in Northeast China is more than 35 million tons, and rice husk accounts for about 20% of the total mass of rice.[1] About 7 million tons of rice husk are produced in Northeast China every year. However, due to the low nutrient content and high ash content of rice husk, it is difficult to be used to prepare feed or fertilizer. Moreover, the bulk density of rice husk is small and it is difficult to transport. Therefore, most of the rice husk can only be burned in situ or abandoned in the field, resulting in serious waste of resources and environmental pollution.[2] With the increasing emphasis on biomass resources and environmental protection, rice husk has been gradually used to replace traditional coal resources for biomass power generation,[3,4] which saves fossil fuels to a certain extent and alleviates the problem of resource waste of rice husk resources. However, the presence of large amounts of alkali metals (K, Na, Si, Ca, Al, and Fe) in rice husk, which are directly used for combustion for power generation, can cause serious problems such as slagging, scaling, and corrosion, which lead to higher maintenance costs.[5] Therefore, the high-value utilization of

Received: September 26, 2024
Revised: November 17, 2024
Accepted: December 4, 2024
Published: December 11, 2024

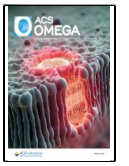

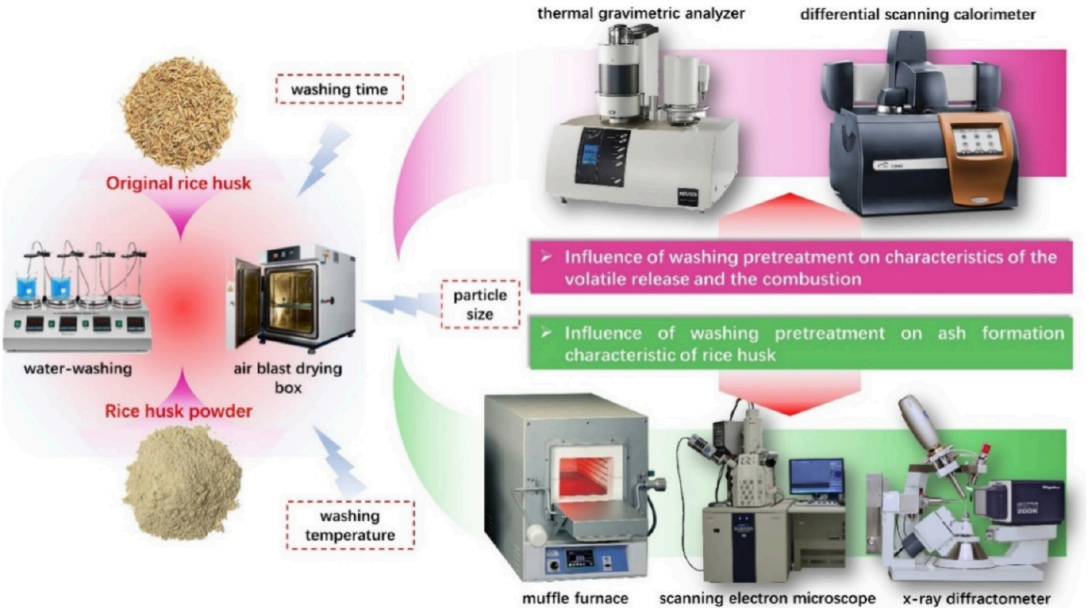

Figure 1. Experimental scheme and research route.

rice husk resources is of great significance for the efficient value-adding of the grain industry in Northeast China and the development of an energy-saving and environmentally friendly circular economy.

Studies have shown that rice husk itself can be used as a raw material for the production of activated carbon[6] and as a soil conditioner to improve soil structure[7] and that biocomposites prepared using rice husk provide an environmentally friendly material for the construction industry.[8] In addition, the application of rice husk in battery electrodes, capacitors, and energy storage materials has received widespread attention.[9] However, due to the high ash content of rice husk, the carbon materials prepared directly have a low specific surface area, which limits their effective application in the agricultural and industry field. Therefore, pretreatment of rice husk is required to effectively utilize the rice husk resource. Common pretreatment methods for rice husk are acid washing,[10] alkali washing,[11] baking,[12] etc. Guo et al.[13] explored the thermal stability of waste incineration fly ash at different heat treatment temperatures (1000−1500 °C). As the heat treatment temperature increased, both the solidification rate and leaching rate of heavy metal Pb decreased. Ma et al.[14] investigated the effect of different inorganic acids (HCl, HF, and H_3PO_4), acid concentrations, and acid washing times on the pyrolysis of rice husk for the preparation of bio-oil and found that the removal rates of K, Ca, Na, and Mg by hydrochloric acid washing reached 98, 93, 100, and 91%, respectively. Hiremath et al.[15] used tartaric acid-modified rice husk as a fluoride ion adsorbent and showed that the maximum adsorption rate of tartaric acid-modified rice husk biomass char could reach 74.73%. Fang et al.[16] discovered that alkali washing pretreatment could increase the yield of volatile fatty acids in rice husk. The total number of volatile fatty acids increased by 72.9%. Meanwhile, some scholars have also improved the effectiveness of the washing pretreatment by combining multiple pretreatment methods. The rice husk was roasted before gasification, resulting in a large amount of H_2 and CO and a small amount of syngas of CO_2 and tar components.[17] The acid treatment of rice husk after alkali treatment can increase the cellulose content by 2.01 times and the crystallinity by 40.8%.[18] Ninduangdee et al.[19] found that blending pelletized rice husk with moisturized rice husk in a fluidized bed could significantly reduce NO_x gas emission. In addition to this, there are several emerging technologies for rice husk pretreatment in recent years, including ultrasonic technology[20] and microbial technology.[21]

The above pretreatment methods affect the physicochemical properties of rice husk from different perspectives and will improve the combustion and ash formation characteristics of rice husk. However, acid or alkaline washing pretreatment requires the use of acidic and alkaline reagents and an additional neutralization step, which not only incurs a high cost but also leads to a large amount of organic matter loss during the treatment process.[22,23] After baking pretreatment, alkali metal removal is not obvious and the problem of slagging and scaling is not effectively improved.[24] Also, although the emerging pretreatment technology has its unique advantages, it has higher requirements for equipment and is more difficult to operate.[25] In contrast, washing pretreatment is widely recognized as a pretreatment technology with obvious advantages due to its low cost and simple operation.[26] The effectiveness of washing depends on the washing temperature, washing time, solid-to-liquid ratio, and particle size.[27,28] The fuel properties of agricultural wastes (wheat straw, rice straw, corn stalk, cotton stalk, candlenut wood, and rice hull) were all improved with increasing washing temperature, and the removal of K and SiO_2 increased with increasing washing temperature.[29] In a study on wheat straw,[30] it was found that the calorific value of washed wheat straw with solid−liquid ratios of 1:50 and 1:10 increased by 16 and 5%, respectively, compared with that of untreated wheat straw. Although small particle size biomass can remove ash more efficiently than large particle size biomass by washing, too small a particle size can also lead to loss of organic matter.[31] For different biomass, changing only a single washing parameter is not effective in removing ash and alkali metals. In this case, multiple washing parameters must be varied to improve the slagging and scaling tendency more effectively. Zhao et al.[32] explored the effects of

https://doi.org/10.1021/acsomega.4c08820
ACS Omega 2024, 9, 50705−50719

three washing temperatures (30, 60, and 90 °C) and three washing times (3, 12, and 24 h) on the pyrolysis of salix under N_2 and CO_2 atmospheres, respectively. The results showed that the removal of elements K, Mg, S, and Cl increased gradually with the increase in washing time and washing temperature, while the removal of K was above 90% and was not significantly affected by time and temperature. Tan et al.[33] studied the removal of element K in palm fiber by changing the washing time (30, 60, and 120 min), solid-to-liquid ratio (1:10, 1:13, and 1:20), and washing temperature (28, 60, and 120 °C). They found that increasing these three washing parameters could effectively remove 73−89% of element K. Singhal et al.[34,35] studied the combustion characteristics and slagging and fouling tendencies of wheat straw under different sizes (3, 1, and 0.05−0.08 cm), different washing times (0, 2, 5, 10, 30, 60, and 180 min), and different washing temperatures (20, 40, 60, and 80 °C). The results showed that long-time washing and increasing the washing temperature could effectively remove the ash content (25−37%) and the contents of alkali metal elements (K (42−55%), Cl (60−81%), S (32−61%), Mg (52−68%), N (17−25%), P (11−37%), and Ca (14−29%)), and the slagging and fouling tendencies were greatly reduced.

In summary, the most researched objects on biomass washing pretreatment are wheat straw, corn stover, forestry waste, etc. Therefore, it is necessary to further study the combustion characteristics and ash formation characteristics of the washed rice husk. Washing time and washing temperature can effectively reduce the tendency of slagging and scaling, while a comparative study of washing on the ash formation and slagging characteristics of unground and ground rice husk has not been involved. Therefore, in this paper, the combustion and ash formation characteristics of rice husk were studied in depth under the conditions of different washing temperatures, washing times, and rice husk particle sizes, which provided a theoretical basis for the high-value utilization of rice husk in Northeast China.

2. EXPERIMENTAL METHODS AND PROCEDURES

2.1. Experimental Platform and Operation. The experimental scheme is shown in Figure 1. The experimental instruments include a washing device, air blast drying box, elemental analyzer (Elementar), thermogravimetric analyzer (Mettler Toledo TGA/SDTA851e), muffle furnace, scanning electron microscope (Quanta 200FEG & EVO18; physical magnification, 500−10,000), and X-ray diffractometer (D8 ADVANCE; the maximum power is 2 kW; the radiation source is Cu target; ±0.0001°).

2.1.1. Washing Preparation of Samples.

1. Six grams of original rice husk/rice husk powder (180 mesh) was weighed. An appropriate amount of water (the washing temperature was 23 or 70 °C; the washing time was 6 or 18 h) was added to ensure the dissolution of soluble substances by using a magnetic stirrer.
2. The rice husk powder was suction-filtered by a vacuum pump after washing. Then, the rice husk powder was placed in a drying oven at 105 °C and dried for 24 h.
3. The original rice husk was dried naturally for 2 days after washing. The rice husk was dried at 105 °C for 24 h and prepared for use.

2.1.2. Preparation and Analysis of Ash. In this article, ash samples were prepared according to the standard (ASTME1755) of American Society for Testing and Materials (ASTM).

1. In a muffle furnace, the rice husk ash was prepared at the temperatures of 600, 815, and 1100 °C.
2. The ash sample was burned to ensure that the mass change after two burns was less than 1 mg, and the final ash quality was determined.

For the convenience of analysis, "TT-HH-F (K)" was used to represent different pretreatment methods. TT represents the washing temperature (°C), HH represents the washing time (h), F indicates that the research object is rice husk powder, and K indicates that the research object is the original rice husk.

2.2. Material Characteristics. In this paper, the rice husk of Shenyang, Liaoning, China, was selected as the research object. According to the elemental analysis standard of coal (GB/T31391-2015), the elemental analysis was carried out, and the calorific value was tested based on the determination method of heat release of solid biomass fuel (GB/T30727-2014) (Table 1).

Table 1. Elemental Analysis and Calorific Value Calculation

parameter	C (%)	H(%)	O[a] (%)	N (%)	S (%)	lower calorific value
rice husk	36.100	5.328	38.602	0.740	0.160	12,934 J/g

[a]Note: calculated by difference (O (%) = 100% − (C + H + N + ash) (%)).[36]

The moisture, ash, volatile matter, and fixed carbon content of rice husk was determined and analyzed by using the muffle furnace according to the national standard of the People's Republic of China-Solid Biomass Fuel Industry Analysis Method (GB/T28731-2012). The following table is the average of three parallel experimental results (Table 2).

Table 2. Proximate Analysis

parameter	moisture (%)	ash (%)	volatile matter (%)	fixed carbon (%)
rice husk	5.39	19.07	65.77	10.31

Air was selected as the environmental atmosphere for the thermogravimetric analysis. The weight of rice husk sample was 10 mg, the environmental gas flow rate was 50 mL/min, and the temperature was increased to 1000 °C at a heating rate of 20 °C/min. The thermogravimetric analysis results are shown in Figure 2. The thermogravimetry (TG) curve could be divided into four stages: The first stage was the drying stage of rice husk, which was from 42 to 119 °C, and the maximum water evaporation rate was at the temperature of 69 °C. The second stage was the preheating stage, which occurred between T = 119 and 240 °C. At this stage, small amounts of biomass hemicellulose (carboxyl and hydroxyl) and other low-molecular-weight substances were decomposed, releasing H_2O, CO, and CO_2. The third stage was the main combustion stage, which occurred at T = 240−500 °C. A large amount of volatile matter was released, and cellulose, hemicellulose, and lignin reacted. At this stage, when the temperature reached the ignition point (T = 280 °C), the surrounding high-temperature air and volatile matter were mixed and burned to further accelerate the release of volatile matter. The volatile matter

https://doi.org/10.1021/acsomega.4c08820
ACS Omega 2024, 9, 50705−50719

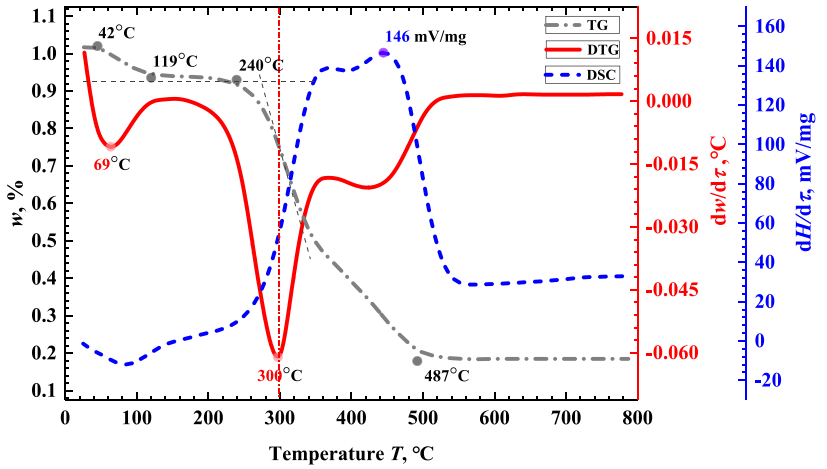

Figure 2. TG, DTG, and DSC of rice husk.

precipitation reached the maximum value at the temperature of T = 300 °C, the mass change rate was 75%, and the maximum weight loss peak was present in the differential TG (DTG) curve. With the increase in temperature, there was an obvious weight loss peak in the DTG curve at about 440 °C, which was due to the massive decomposition of lignin and the reaction of a large number of gaseous products with coke.[37] At the same time, the alkali metals in the biomass turned to the molten state, the absorption/exothermic reaction existed at the same time, and the differential scanning calorimetry (DSC) curve showed a double-peak structure ($(dH/d\tau)_{max}$ = 146 mV/mg). The fourth stage was the fixed carbon reaction stage, which occurred at $T \geq$ 500 °C. At this time, the remaining small amounts of lignin and residues continue to decompose slowly,[38] and the DTG curve tends to be stable.

3. RESULTS AND ANALYSIS

3.1. Effects of Washing Pretreatment on Volatile Matter Release and Combustion Characteristics. In this article, the comprehensive characteristic index of volatile release D represents the volatile matter release characteristics and the difficulty of the reaction. The average combustion rate

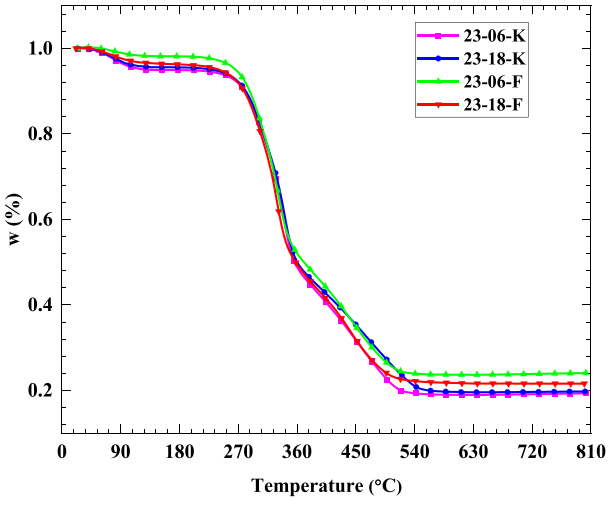

Figure 3. TG analysis of rice husk/rice husk powder with the washing time of 6/18 h and washing temperature of 23 °C.

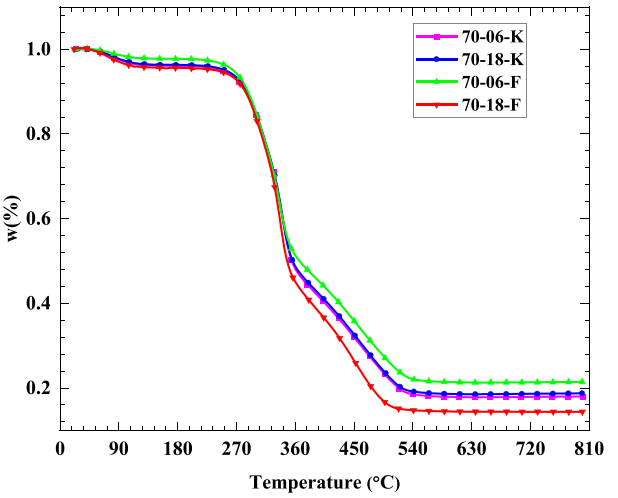

Figure 4. TG analysis of rice husk/rice husk powder with the washing time of 6/18 h and washing temperature of 70 °C.

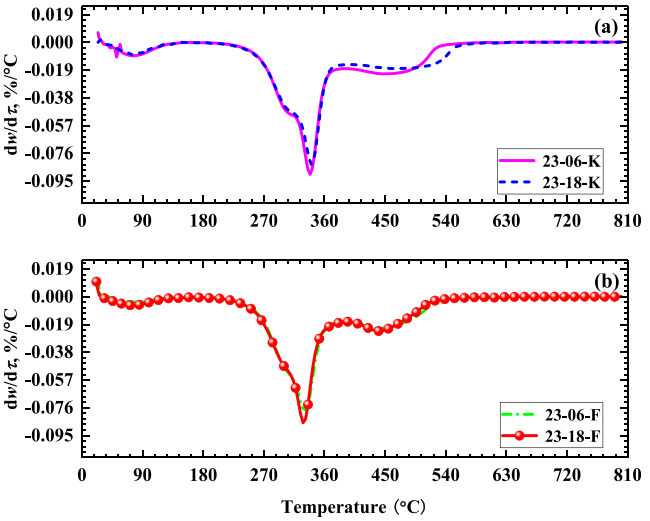

Figure 5. DTG analysis of rice husk/rice husk powder with the washing time of 6/18 h and washing temperature of 23 °C. (a) Original rice husk; (b) rice husk powder.

v_{mean} was used to reflect the intensity of the combustion process.[39,40] The formula is as follows:

https://doi.org/10.1021/acsomega.4c08820
ACS Omega 2024, 9, 50705−50719

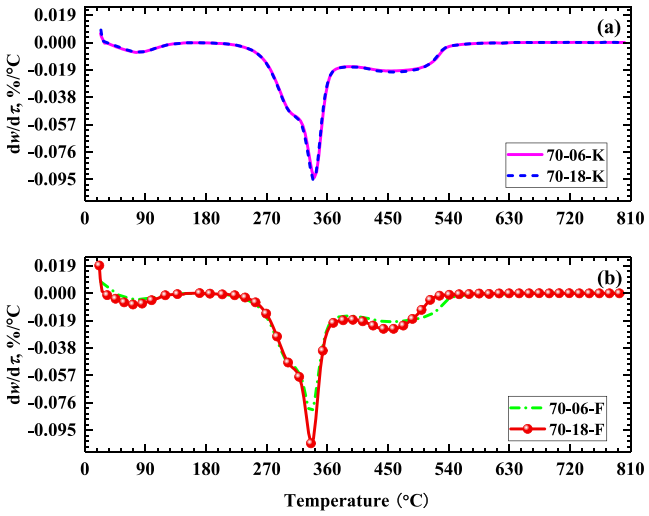

Figure 6. DTG analysis of rice husk/rice husk powder with the washing time of 6/18 h and washing temperature of 70 °C. (a) Original rice husk; (b) rice husk powder.

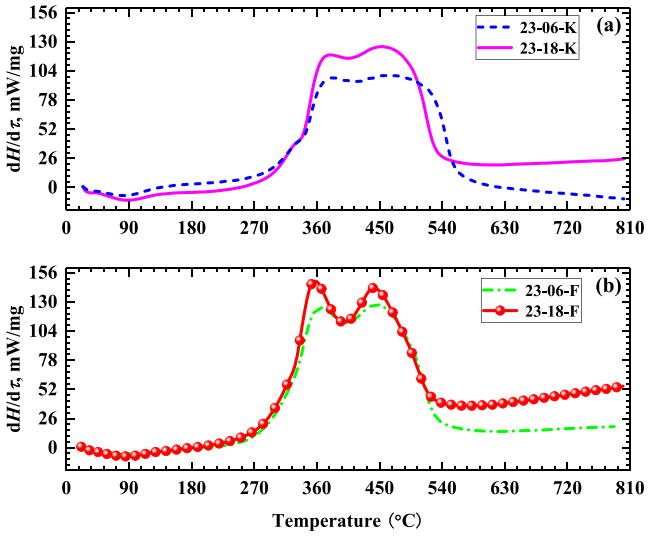

Figure 7. DSC analysis of rice husk/rice husk powder with the washing time of 6/18 h and washing temperature of 23 °C. (a) Original rice husk; (b) rice husk powder.

$$D = \frac{(\mathrm{d}w/\mathrm{d}\tau)_{max}(\mathrm{d}w/\mathrm{d}\tau)_{mean}}{T_s \cdot T_{max} \cdot \Delta T_{1/2}} \quad (1)$$

$$\nu_{mean} = \beta \times \frac{\alpha_s - \alpha_f}{T_f - T_s} \quad (2)$$

where $(\mathrm{d}w/\mathrm{d}\tau)_{max}$ is the maximum weight loss rate (%/°C). $(\mathrm{d}w/\mathrm{d}\tau)_{mean}$ is the average weight loss rate (%/°C). T_s is the volatile devolatilization initial temperature (°C). T_{max} is the temperature corresponding to the maximum weight loss rate (°C). $\Delta T_{1/2}$ is the temperature range corresponding to $(\mathrm{d}w/\mathrm{d}\tau)/(\mathrm{d}w/\mathrm{d}\tau)_{max} = 1/2$ (°C). ν_{mean} is the average burning rate (%/min). T_f is the burnout temperature (°C). β is the heating rate (°C/min). α_s is the mass fraction of the sample on fire (%). α_f is the mass fraction of the sample at burnout (%).

At the same time, the combustion characteristic index represented the combustion reaction change of rice husk. The combustion characteristic index mainly included the flammability index C_r, ignition characteristic index C_i, and comprehensive combustion characteristic index S.[41−43] The formulas of each index were as follows:

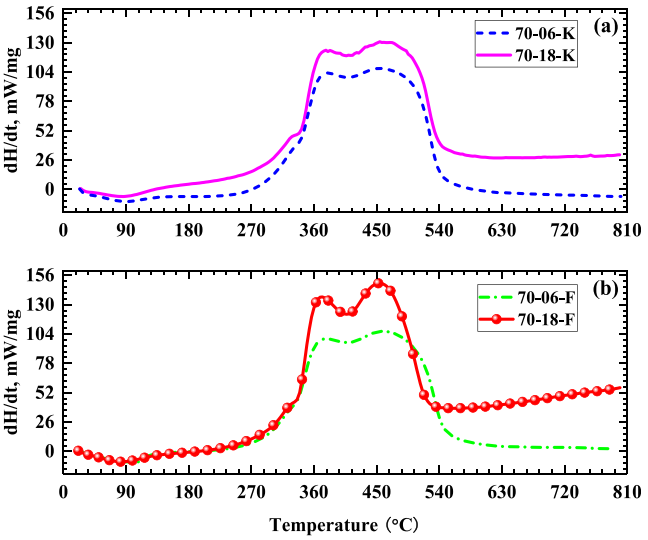

Figure 8. DSC analysis of rice husk/rice husk powder with the washing time of 6/18 h and washing temperature of 70 °C. (a) Original rice husk; (b) rice husk powder.

$$C_r = \frac{(\mathrm{d}w/\mathrm{d}\tau)_{max}}{T_s^2} \quad (3)$$

$$C_i = \frac{V_{ad} \cdot (\mathrm{d}w/\mathrm{d}\tau)_{max}}{T_s} \quad (4)$$

$$S = \frac{(\mathrm{d}w/\mathrm{d}\tau)_{max} \cdot \nu_{mean}}{T_s^2 T_f} \quad (5)$$

where V_{ad} is analysis-based volatile matter (%).

From Figures 3 and 4, it can be seen that under the condition of high washing temperature, adjusting the washing time could significantly change the combustion characteristics of rice husk powder. Compared with the shorter washing time (t = 6 h), prolonging the washing time (t = 18 h) increased the ignition temperature. As shown in Figures 5 and 6, changing the particle size of rice husk could affect the temperature corresponding to the maximum weight loss rate T_{max}. Under the same conditions, the T_{max} of washed rice husk powder and washed rice husk could differ by 5−10 °C ($T_{max,23\text{-}X\text{-}k}$ = 338 °C; $T_{max,23\text{-}X\text{-}F}$ = 328 °C; $T_{max,70\text{-}X\text{-}k}$ = 340 °C; $T_{max,70\text{-}X\text{-}F}$ = 335 °C). In addition, whether under high or low washing temperature, for the original rice husk, the longer the washing time was, the more unfavorable it was to increase the maximum weight loss rate $(\mathrm{d}w/\mathrm{d}\tau)_{max}$, $|(\mathrm{d}w/\mathrm{d}\tau)_{max,23\text{-}18\text{-}k}|$ = 0.081%/°C < $|(\mathrm{d}w/\mathrm{d}\tau)_{max,23\text{-}06\text{-}k}|$ = 0.09%/°C). For rice husk powder, the longer the washing time, the higher $(\mathrm{d}w/\mathrm{d}\tau)_{max}$, $|(\mathrm{d}w/\mathrm{d}\tau)_{max,23\text{-}06\text{-}F}|$ = 0.077%/°C < $|(\mathrm{d}w/\mathrm{d}\tau)_{max,23\text{-}18\text{-}F}|$ = 0.086%/°C) (as shown in Figure 5); especially under the condition of high washing temperature, the volatile matter release rate of rice husk powder increased significantly in the combustion stage ($|(\mathrm{d}w/\mathrm{d}\tau)_{max,70\text{-}18\text{-}F}|$ = 0.104%/°C). As shown in Figures 7 and 8, compared with the shorter washing time, prolonging the washing time will lead to an increase in heat absorption, indicating that the exothermic reaction was promoted. In addition, for rice husk powder, a steep trough was formed between the two endothermic peaks of the DSC

https://doi.org/10.1021/acsomega.4c08820
ACS Omega 2024, 9, 50705−50719

Table 3. Characteristic Parameters

condition	T_s (°C)	T_{max} (°C)	$(dw/d\tau)_{max}$ (%/°C)	T_f (°C)	D (−)	S (−)	C_r (−)	C_i (−)
original	240.00	300.00	6.11	494.1	3.37×10^{-7}	1.09×10^{-6}	8.63×10^{-5}	0.144
23-06-F	286.62	332.34	8.00	505.4	6.42×10^{-7}	1.31×10^{-6}	9.74×10^{-5}	0.190
23-06-K	299.05	338.65	9.02	517.1	5.89×10^{-7}	1.36×10^{-6}	1.01×10^{-4}	0.210
23-18-F	288.37	330.12	8.67	503.8	6.25×10^{-7}	1.43×10^{-6}	1.04×10^{-4}	0.208
23-18-K	301.20	340.34	8.33	544.7	4.43×10^{-7}	1.05×10^{-6}	9.18×10^{-5}	0.173
70-06-F	291.53	335.86	8.20	527.7	5.89×10^{-7}	1.10×10^{-6}	9.65×10^{-5}	0.173
70-06-K	301.78	340.74	9.36	537.4	4.19×10^{-7}	1.35×10^{-6}	1.03×10^{-4}	0.215
70-18-F	301.08	336.60	10.54	505.1	10.6×10^{-7}	1.83×10^{-6}	1.16×10^{-4}	0.278
70-18-K	302.50	338.91	9.52	527.8	6.17×10^{-7}	1.36×10^{-6}	1.04×10^{-4}	0.218

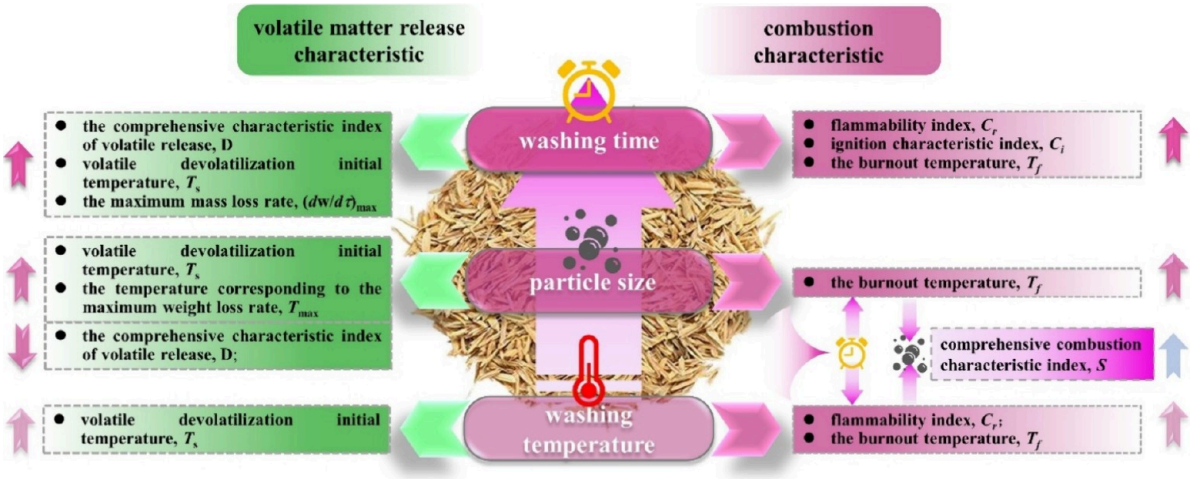

Figure 9. Effects of different washing conditions (washing time, washing temperature, and particle size) on the comprehensive characteristics of volatile release and combustion characteristics.

Table 4. Expressions of Several Common Solid-Phase Reaction Dynamics Models[47a]

model		$G(\alpha)$ function	symbol	correlation coefficient $\overline{R}^2$
chemical reaction control model	level 1 reaction	$-\ln(1-\alpha)$	F1	0.9210
	level 3/2 reaction	$2[(1-\alpha)^{-1/2}] - 1$	F3/2	0.3830
	level 2 reaction	$(1-\alpha)^{-1} - 1$	F2	0.9262
	level 3 reaction	$[(1-\alpha)^{-2} - 1]/2$	F3	0.9220
	level 4 reaction	$[(1-\alpha)^{-3} - 1]/3$	F4	0.9194
diffusion control model	one-dimensional diffusion	α^2	D1	0.9903
	two-dimensional diffusion	$(1-\alpha)\ln(1-\alpha) + \alpha$	D2	0.9934
	three-dimensional diffusion, spherical symmetry	$[1-(1-\alpha)^{1/3}]^2$	D3	0.9389
	three-dimensional diffusion, cylindrical symmetry	$[1-(2/3)\alpha] - (1-\alpha)^{2/3}$	D4	0.8971

[a]Note: $\overline{R}^2 = (R_1^2 + R_2^2)/2$, where R_1^2 and R_2^2 are the correlation coefficients of $n[G(\alpha)/T^2]$ and $1/T$ relationship curves in the temperature ranges of 250−335 and 335−480 °C, respectively.

curve after prolonging the washing time, indicating that the endothermic/exothermic reactions were frequent, the transition of alkali metals to the molten state was more active in the combustion reaction, and a large number of gaseous products reacted with fixed carbon. Therefore, the coupling effect of washing temperature and washing time on the combustion characteristics of rice husk was obvious. The coupling effect of particle size and washing time on the comprehensive characteristics of volatile release was obvious. Long washing time was more beneficial to improve the combustion characteristics of rice husk and promoted the increase of rice husk calorific value.

According to the TG, DTG, and DSC analyses and eqs 1−5, the comprehensive characteristics of volatile release and combustion characteristic index of rice husk samples with/without washing were obtained. The calculation results are shown in Table 3. In Table 3, the comprehensive characteristics of volatile release and combustion characteristics of rice husk with and without washing were compared. Because the water-soluble alkali metals in the original rice husk were removed by washing pretreatment, the combustion reaction rate slowed down, and the T_s had been significantly increased, indicating that more heat was required to reach the volatile devolatilization initial temperature. Therefore, the volatile matter release occurred with a delay, and the comprehensive characteristic index of volatile release (D) increases significantly. However, although it was not easy for the rice husk after washing to quickly enter the combustion reaction state, the combustion stability of the washed rice husk was greatly improved, the burnout time was delayed, and the T_f was

https://doi.org/10.1021/acsomega.4c08820
ACS Omega 2024, 9, 50705−50719

Table 5. Kinetic Parameters of Rice Husk with the Washing Pretreatment

sample	temperature (°C)	fitting equation $y = ax + b$ a	b	activation energy E (kJ/mol)	frequency factor A (min^{-1})	correlation coefficient R^2
original rice husk	250−335	−11,546.942	4.7190	96.007	2.59×10^{4}	0.9916
	335−480	−2665.493	−9.9240	22.162	2.61×10^{-3}	0.9951
23-06-F	235−350	−16,971.500	13.001	141.11	1.50×10^{8}	0.9911
	350−495	−2798.060	−9.8560	23.264	2.93×10^{-3}	0.9936
23-18-F	240−345	−14,148.038	8.4620	117.64	1.34×10^{6}	0.9843
	345−507	−2709.658	−9.9330	22.530	2.63×10^{-3}	0.9939
70-06-F	240−355	−16,495.371	12.0910	137.150	5.88×10^{7}	0.9915
	355−530	−2479.364	−10.402	20.615	1.51×10^{-3}	0.9925
70-18-F	240−355	−15,542.834	10.530	129.230	1.16×10^{7}	0.9867
	355−540	−2785.090	−9.8370	23.157	2.98×10^{-3}	0.9896
23-06-K	250−355	−13,855.354	7.7420	115.20	6.38×10^{5}	0.9894
	355−520	−2627.961	−10.111	21.850	2.14×10^{-3}	0.9941
23-18-K	247−360	−13,690.253	7.4090	113.83	4.52×10^{5}	0.9910
	360−555	−2205.484	−10.814	18.337	8.87×10^{-4}	0.9911
70-06-K	250−357	−15090.524	9.7010	125.47	4.93×10^{6}	0.9916
	357−532	−2387.744	−10.488	19.853	1.33×10^{-3}	0.9934
70-18-K	248−360	−15339.978	10.106	127.54	7.52×10^{6}	0.9914
	360−530	−2452.237	−10.399	20.389	1.49×10^{-3}	0.9919

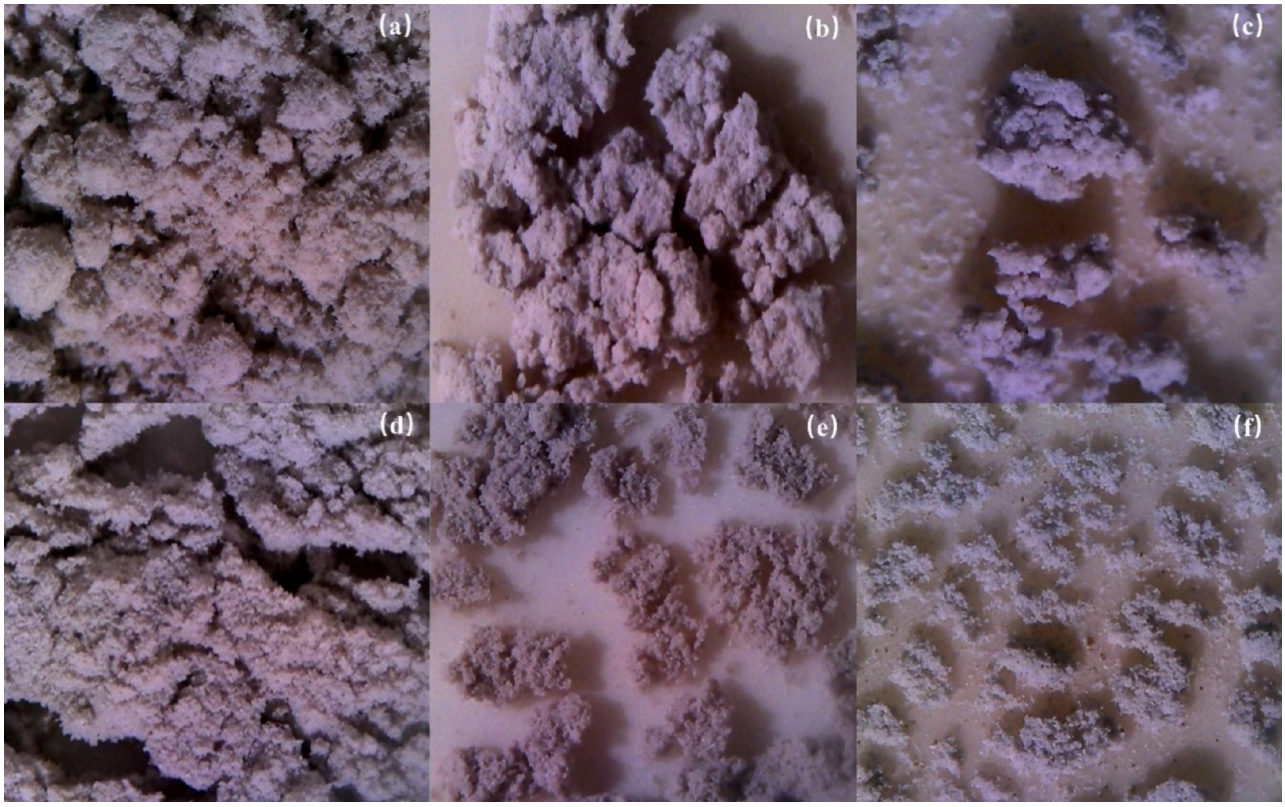

Figure 10. (a) Sintering temperature of 600 °C, original rice husk (1.6×); (b) sintering temperature of 815 °C, original rice husk (1.6×); (c) sintering temperature of 1100 °C, original rice husk (1.6×); (d) sintering temperature of 600 °C, 70-18-K (1.6×); (e) sintering temperature of 815 °C, 70-18-K (1.6×); (f) sintering temperature of 1100 °C, 70-18-K (1.6×).

significantly improved, which could be verified by the increase in C_r and C_i of the washed rice husk (see Table 3). In addition, the overall porosity of rice husk increased after washing,[44] and the channels were smooth for volatile matter release, resulting in an increase the maximum weight loss rate $(dw/d\tau)_{max}$.

The flammability index C_r, burnout temperature T_f, and volatile devolatilization initial temperature T_s were all sensitive to the washing temperature. With the increase in washing temperature, the above three parameter values increased obviously. The particle size d of washed rice husk was positively correlated with the T_s, T_{max}, and T_f. Therefore, D was closely related to the particle size of washed rice husk, and the two were negatively correlated. In addition, C_r and C_i were affected by the particle size and washing temperature. With the increase in the washing time, the smaller particle size showed a larger integrated combustion property index (S), but in the

https://doi.org/10.1021/acsomega.4c08820
ACS Omega 2024, 9, 50705−50719

Table 6. Ash Content of Rice Husk at Different Sintering Temperatures (600, 815, and 1100 °C)[a]

	600 °C		815 °C		1100 °C	
	proportion of ash formation, M_a (%)	ratio to original ash content, M_t (%)	proportion of ash formation, M_a (%)	ratio to original ash content, M_t (%)	proportion of ash formation, M_a (%)	ratio to original ash content, M_t (%)
original sample	20.68	100	19.9	100	18.3	100
70-18-K	17.58	85.01	16.82	84.52	16.67	91.09

[a]Note: rice husk without washing, M_a = ash mass/sample mass, M_t = ash mass/ash content from the rice husk without washing; rice husk with washing (70-18-K), M_a = ash mass/sample mass with washing, M_t = ash mass/ash content from the rice husk without washing.

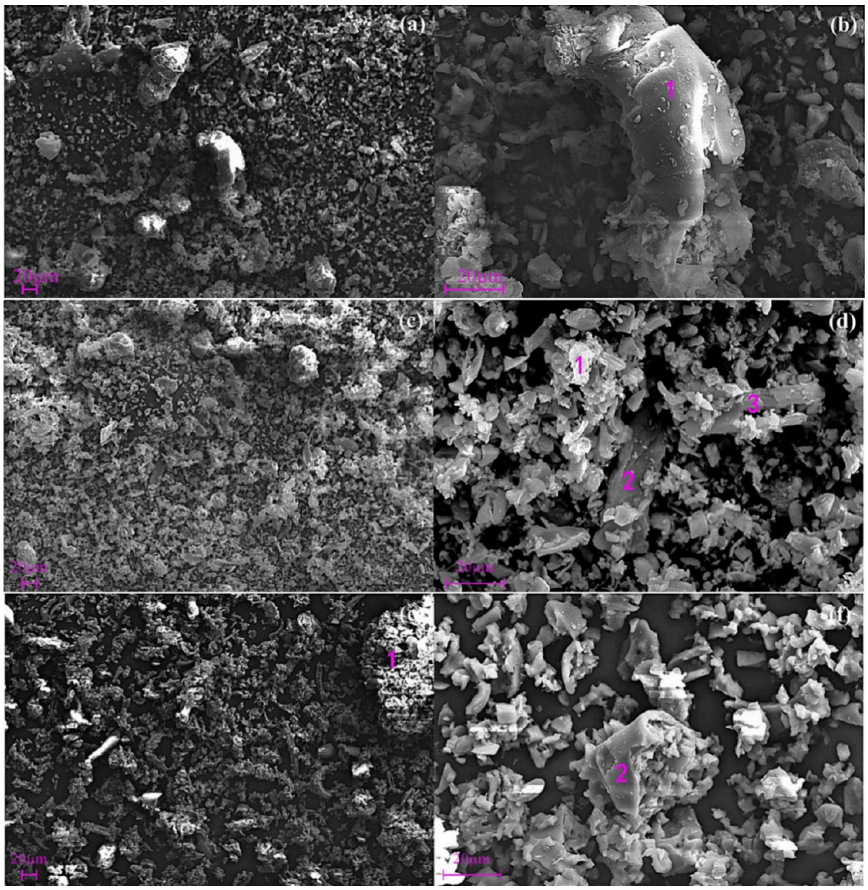

Figure 11. Microstructure of original rice husk ash at different sintering temperatures: (a, b) 600 °C, (c, d) 815 °C, and (e, f) 1100 °C.

Table 7. Elemental Analysis for the Different Measuring Points of Rice Husk Ash by SEM (EDS)

		mass fraction of main elements (%)					
	measuring point	C	Si	O	K	Fe	Ca
600 °C	1		53.3	34.74	5.69		
815 °C	1		34.68	55.88	4.11		1.03
	2		66.09	19.73	4.88	4.67	
	3		43.18	45.54	0.3	1.83	
1100 °C	1		43.93	51.6	1.17		
	2		42.47	50.1			

shorter washing time, the original rice husk presented better combustion characteristics. The above law was particularly obvious under high temperature washing conditions ($\Delta S_{23} = S_{23\text{-}18\text{-}F} - S_{23\text{-}18\text{-}K} = 0.38 \times 10^{-6} < \Delta S_{70} = S_{70\text{-}18\text{-}F} - S_{23\text{-}18\text{-}F} = 0.47 \times 10^{-6}$). This paper considers that it was mainly due to the fact that high-temperature washing was more conducive to the release of water-soluble alkali from the inside of biomass and accelerated the desorption effect. However, long washing time led to ion exchange between water-soluble alkali metals and rice husk, forcing alkali metals to be rehosted by rice husk. Furthermore, the aggregation effects of rice husk powder could promote the enrichment of alkali metals and simplify some steps of alkali metals participating in combustion reactions so that alkali metals could fully and quickly participate in the combustion reaction from the beginning. In summary, the relationship among the influencing factors (washing time, washing temperature, and particle size), comprehensive characteristics of volatile release, and combustion characteristics is shown in Figure 9.

The reaction kinetic parameters obtained by thermogravimetric analysis can macroscopically describe the whole chemical reaction process of biomass. Under the condition of ignoring the secondary products of gas, without considering the heat and mass transfer caused by the material concentration diffusion, according to the Arrhenius equation, the reaction rate can be expressed as:[45,46]

https://doi.org/10.1021/acsomega.4c08820
ACS Omega 2024, 9, 50705−50719

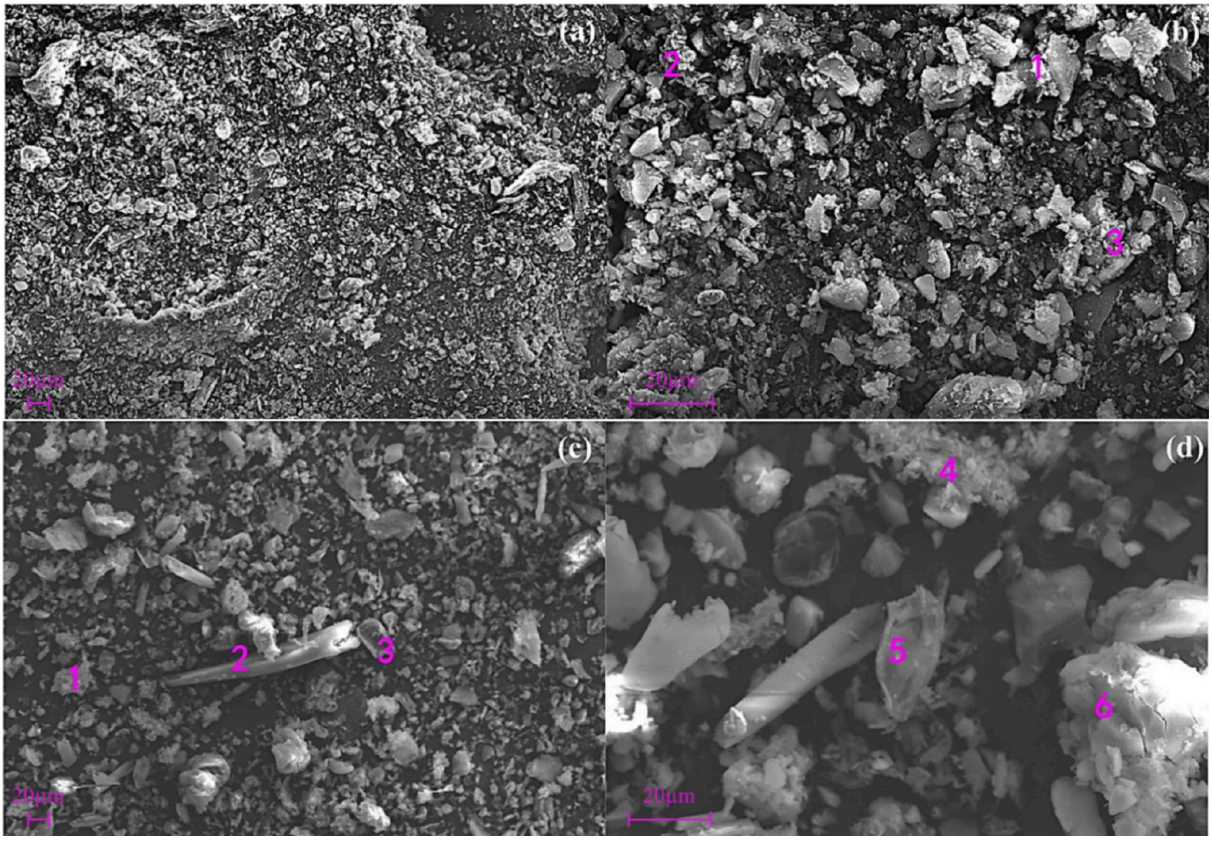

Figure 12. Microstructure of the ash sample at a sintering temperature of 600 °C. (a) 23-18-K, 500×; (b) 23-18-K, 2.00k×; (c) 23-18-F, 500×; (d) 23-18-F, 2.00k×.

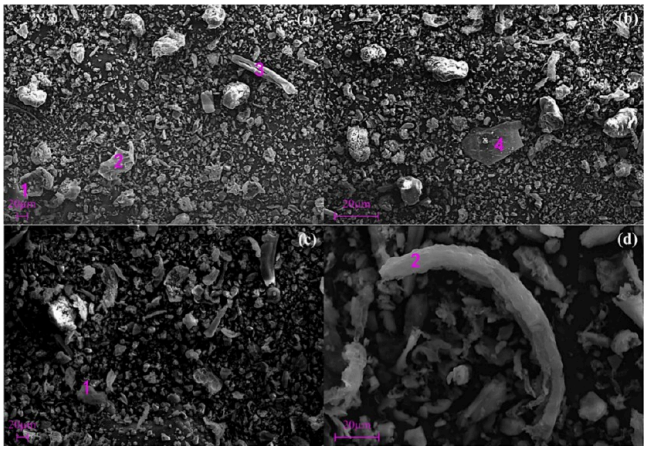

Figure 13. Microstructure of the ash sample at a sintering temperature of 815 °C. (a) 23-18-K, 500×; (b) 23-18-K, 2.00k×; (c) 23-18-F, 500×; (d) 23-18-F, 2.00k×.

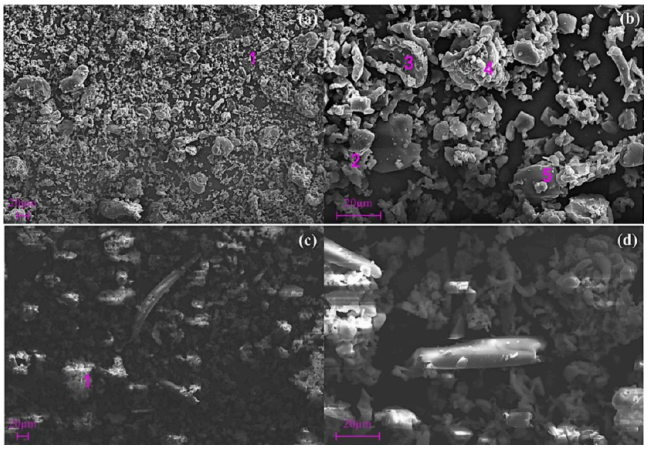

Figure 14. Microstructure of the ash sample at a sintering temperature of 1100 °C. (a) 23-18-K, 500×; (b) 23-18-K, 2.00k×; (c) 23-18-F, 500×; (d) 23-18-F, 2.00k×.

$$\frac{d\alpha}{dt} = kf(\alpha) \tag{6}$$

$$k = A\exp\left(-\frac{E}{RT}\right) \text{ and } \alpha = \frac{m_0 - m}{m_0 - m_\infty} \tag{7}$$

$$\ln\left[\frac{G(\alpha)}{T^2}\right] = \ln\frac{AR}{\beta E} - \frac{E}{RT} \tag{8}$$

where R is the gas constant (R = 8.3145 J/(mol K)), T is the instantaneous temperature (K), E is the activation energy (kJ/mol), and A is the frequency factor (min^{-1}). α is the weight loss rate (α = 0.15−0.9) (%). m_0 is the initial mass (g). m is the instantaneous mass in the thermogravimetric experiment (g). m_∞ is the residual mass after thermogravimetric experiment (g).

Table 4 shows nine common mechanism functions, $G(\alpha)$. It could be seen from eq 6 and Table 4 that there were different relationship curves of $\ln[G(\alpha)/T^2]$ and $1/T$ corresponding to the different $G(\alpha)$. Through the determined $G(\alpha)$, activation energy E and frequency factor A could be obtained. To ensure the accuracy of the data, the stage with relatively stable test

https://doi.org/10.1021/acsomega.4c08820
ACS Omega 2024, 9, 50705−50719

Table 8. Elemental Analysis for the Different Measuring Points of Rice Husk Ash by SEM (EDS) (23-18-K)

		mass fraction of main elements (%)							
	measuring point	C	Si	O	K	Fe	Ca	Mg	Mn
600 °C	1		36.54	46.39	0.66	1.89	0.83		
	2		28.22	45.75	1.43		3.28	1.62	
	3		34.3	55.5	0.9				
815 °C	1	26.08	35.7	31.25	4.81				
	2		54.45	40.9	0.91				
	3		35.67	58.24			0.53		
	4		43.9	49.86		1.41			
1100 °C	1		37.57	46.21	1.1	2.98	3.85	0.85	
	2		50.04	41.78					
	3	13.72	42.69	34.9		1.49			
	4		37.01	54.5		1.01			
	5		23.27	37.5	0.96	24.79			

Table 9. Elemental Analysis for the Different Measuring Points of Rice Husk Ash by SEM (EDS) (23-18-F)

		mass fraction of main elements (%)							
	measuring point	C	Si	O	K	Fe	Ca	Mg	Mn
600 °C	1		67.17	32.83					
	2	53.17	12.15	33.65	0.22		0.58	0.25	
	3		33.29	59.30	0.85	2.06	1.48	0.79	
815 °C	1	46.41	16.47	35.16	0.32				
	2		38.42	54.87			0.57		
1100 °C	1		39.77	54.79		2.46	1.44		1.54

conditions should have been selected for activation energy calculation. In addition, the relationship curve of $\ln[G(\alpha)/T^2]$ and $1/T$ could be divided into two temperature ranges, which represent the volatilization stage and the combustion stage of fixed carbon. It could be seen from Figure 1 and Table 4 that when the expression of $G(\alpha)$ was D2 model, the correlation coefficient $\overline{R}^2$ was the closest to 1. Therefore, the D2 model "$G(\alpha) = (1 - \alpha)\ln(1 - \alpha) + \alpha$" was selected to calculate the kinetic parameters.

As shown in Table 5, the activation energies of rice husk in the volatile matter release stage and fixed carbon combustion stage were 96.007 and 22.162 kJ/mol, respectively. It could be seen that the activation energy in the first stage (the volatile matter release stage) was much larger than that in the second stage (the fixed carbon combustion stage). This was mainly due to the fracture of the biomass macromolecular chain in the biomass in the first stage, which needed to provide higher energy. In the second stage, with increasing temperature, rice husk was more likely to react (the release of CO and H_2 requires less energy). Therefore, the average activation energy of rice husk in the high temperature range was lower than that in the low temperature range.

Because washing removed some alkali metal elements in rice husk that could promote pyrolysis, it was difficult for volatile matter release. Therefore, in the first stage, the heat consumed by the biomass combustion reaction increased, and the average activation energy of washed rice husk in the first stage was 125.896 kJ/mol, which was much larger than that of the original rice husk in this stage. In the second stage, the activation energy of biomass did not change much. The minimum activation energy was 18.337 kJ/mol, and the maximum activation energy was 23.264 kJ/mol. In general, the difference of activation energy between the fixed carbon combustion stage and the volatile release stage of the washed rice husk was significantly increased, which was greatly affected by the particle size and was less affected by the washing temperature.

3.2. Effect of Washing Treatment on Ashing Characteristics of Rice Husk. The ash samples were prepared in a muffle furnace at three sintering temperatures of 600, 815, and 1100 °C, and the microstructure characteristic and component change of the ash samples were observed to explore the effect of washing on the ash formation characteristics of rice husk, as shown in Figure 10. Figure 10a–c shows the ash samples of rice husk without washing at three sintering temperatures, respectively. Figure 10a–c shows the ash samples of washed rice husk (70-18-K) at three sintering temperatures, respectively. When the sintering temperature was 600 °C (as shown in Figure 10a), the viscosity of rice husk ash was low, and its structure was loose. At the sintering temperature of 600–800 °C, the SiO_2 in rice husk ash basically existed in an amorphous state. When the sintering temperature was 815 °C (as shown in Figure 10b), the adhesion of rice husk ash was significantly improved, and the ash sample was adhered to the combustion boat. It showed an obvious granular structure and agglomerated and slagged. When the sintering temperature was higher than 900 °C, the appearance of rice husk ash was white (as shown in Figure 10c). When the sintering temperature was 1100 °C (as shown in Figure 10c), the ash adhesion of rice husk ash was further improved, and the ash samples were agglomerated into blocks. In Figure 10d–f, the structure of ash samples from washed rice husk was relatively loose. Even at a higher sintering temperature (1100 °C), the agglomeration degree of ash samples was significantly lower than that of ash samples from unwashed rice husk.

As shown in Table 6, at different sintering temperatures (600, 815, and 1100 °C), the ash content of washed rice husk was about 15% lower than that of the rice husk without washing. At the same time, in the high-temperature sintering stage (1100 °C), the ash content of rice husk without washing

https://doi.org/10.1021/acsomega.4c08820
ACS Omega 2024, 9, 50705–50719

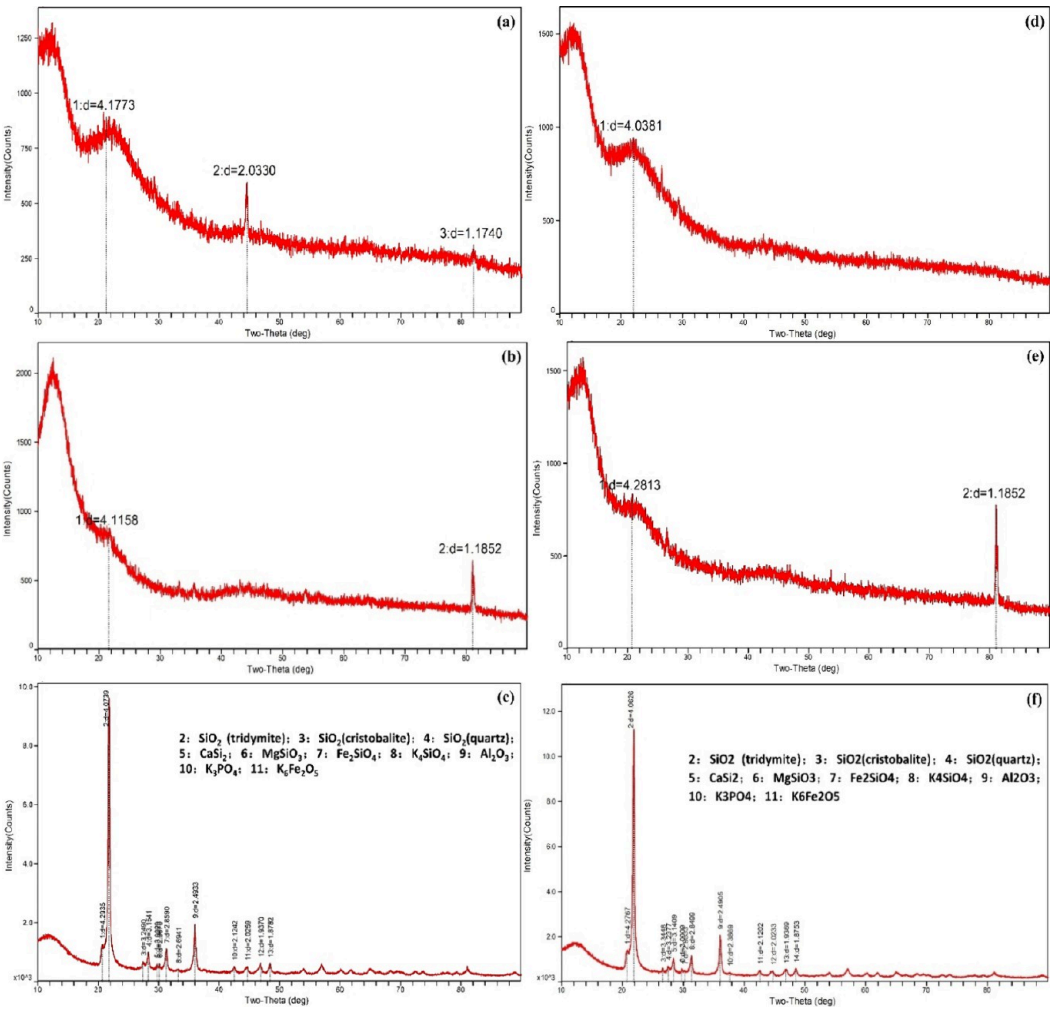

Figure 15. XRD patterns of rice husk ash: (a) sintering temperature of 600 °C (23-18-K), (b) sintering temperature of 815 °C (23-18-K), (c) sintering temperature of 1100 °C (23-18-K), (d) sintering temperature of 600 °C (23-18-F), (e) sintering temperature of 815 °C (23-18-F), and (f) sintering temperature of 1100 °C (23-18-F).

showed a continuous decreasing trend as the sintering temperature increased, while the attenuation of the ash content of rice husk with washing was limited. Therefore, washing pretreatment is helpful to reduce the ash content of rice husk. In a certain temperature range, the ash content of washed rice husk did not change significantly, which made it possible to control slagging through a reasonable temperature range in engineering applications.

The microstructure of rice husk ash was further analyzed by SEM, as shown in Figure 11a. The ash particle outline of rice husk without washing was clear at 600 °C, and there was no obvious adhesion between each other. There were a certain number of unburned large particles that retained the original structure of rice husk (as shown in Figure 11b). There was a thick and rough shell (see the symbol "1" in Figure 11b), the surface was attached with small protrusions, and the flaky particles was in the inner side. With the SEM (energy-dispersive X-ray spectroscopy (EDS)) analysis, it could be seen that the main component of most adhesions on "1" is Si, and the flaky particles on the inner side of the shell were mainly composed of a large number of nanosized amorphous SiO_2, as shown in Table 7.

When the sintering temperature reached about 815 °C, the particle size of rice husk ash decreased obviously, as shown in Figure 11c. Most of the particles were in the glassy state, and agglomeration occurred between some particles, as shown in Figure 11d. When the temperature rose to 1100 °C, the particle size of ash particles decreased further, and the agglomeration between particles was more obvious, as shown in Figure 11e. It could be found from the cross sections of some large particles that the honeycomb structure was present inside the particles, which might have been caused by the volatile release, as shown in Figure 11f. As shown in Table 7, the kalium in ash gradually decreased, indicating that alkali metals gradually precipitated to the ash surface with the increase in sintering temperature. This kind of alkali metal (K) played a significant role in promoting the ash particle agglomeration of rice husk without washing.

As shown in Figures 12−14, after a long time of washing, the ash particles were obviously individualized at the sintering temperature of 600 °C, the particle size was small and relatively uniform, and most of them present a single block structure. With increasing ashing temperature, the agglomeration of particles was improved to a certain extent at the sintering temperature of 815 °C compared to that without washed rice husk ash. When the sintering temperature was 1100 °C, the ash deposit and slagging phenomenon still existed. Under the same conditions of washing temperature

https://doi.org/10.1021/acsomega.4c08820
ACS Omega 2024, 9, 50705−50719

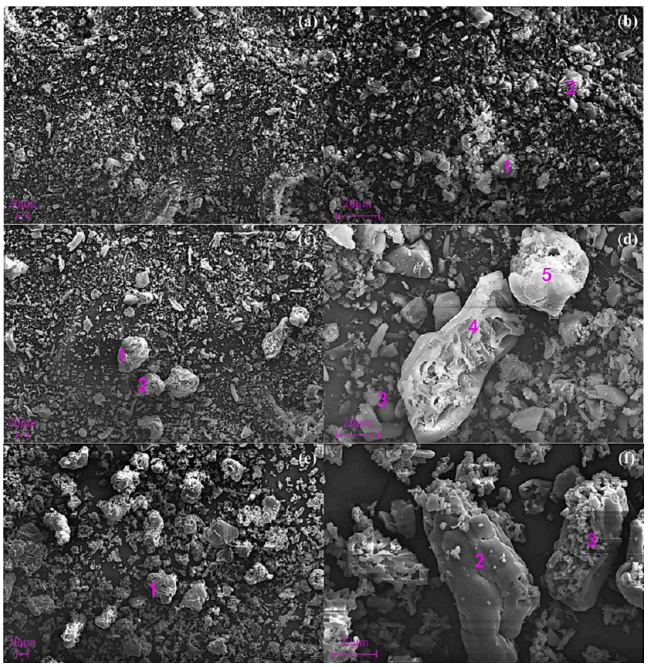

Figure 16. Microstructure of the ash sample at different sintering temperatures (70-18-K): (a, b) 600 °C, (c, d) 815 °C, and (e, f) 1100 °C.

and time, the agglomeration phenomenon of rice husk powder with washing obviously disappeared at higher sintering temperature. On the one hand, it was due to the difference in the morphology of the original rice husk and powder. On the other hand, it was due to the difference in the removal effect of alkali metals after washing (as shown in Tables 8 and 9). During the washing process, the water-soluble alkali metal elements (in ionic and granular mineral forms) in rice husk were first removed by ion diffusion. However, with the extension of washing time, the alkali metals that had been dissolved in the washing solution would have an ion exchange with the rice husk, and the surface structure of the ungrounded rice husk was more likely to adsorb ions and impurities, resulting in the K content in the sintered ash of ungrounded rice husk being higher than that of the rice husk powder with the same washing time and temperature.

In summary, the washing pretreatment could improve the ash deposit and slagging phenomenon of rice husk in the high-temperature sintering stage, but due to the morphology influence of rice husk, the improvement of washing pretreatment on the sintering slagging phenomenon of rice husk powder was more obvious.

From the above SEM (EDS) (Tables 8 and 9) and XRD (Figure 15) analyses, it could be seen that the rice husk ash particles were mainly composed of C, Si, O, K, Fe, Ca, Mg, and Al. The silica in rice husk ash mainly existed in the form of cristobalite. When the sintering temperature was 600 °C, the content of cristobalite increased with increasing temperature. The rice husk ash mainly contained amorphous SiO_2. When the sintering temperature was about 815 °C, the peak value of amorphous SiO_2 in rice husk ash decreased obviously. When the sintering temperature was about 1100 °C, the amorphous silica present in rice husk ash transforms into crystalline tridymite, and the high-temperature refractory Mg−Fe−Al acid salt was formed by the Mg, Fe, and Al components. By comparing the washed rice husk and washed rice husk powder, it was found that the washing pretreatment had a better effect on the removal of alkali metals in rice husk powder. The ash quality decreased significantly; correspondingly, the proportion of refractory silicates increased. The proportion of crystalline tridymite in the sintered ash of rice husk powder was significantly higher than that of rice husk after washing pretreatment.

Under the same washing time (t = 18 h), the washing temperature had a great influence on the microstructure of rice husk ash (Figure 16). From Table 10, it could be seen that under the condition of high washing temperature (70 °C), rice husk ash particles were more dispersed and individualized. In addition, the high washing temperature played a greater role in the removal of alkali metals. When the sintering temperature was 600 °C, the K in rice husk ash accounted for a relatively small proportion, as shown in Table 10. When the sintering temperature was higher than 800 °C, the content of K in rice husk ash was almost not detected. When the sintering temperature was 1100 °C, the proportion of high-temperature refractory Mg−Fe−Al acid salt increased (as shown in Figure 17), which effectively raised the ash melting point and reduced the possibility of ash deposition. Therefore, under the same washing time, the higher washing temperature had a great promoting effect on the removal of alkali metals and the formation of infusible silicates in rice husk ash.

4. CONCLUSIONS

1. Under the condition of high washing temperature, adjusting the washing time could significantly change the combustion characteristics of rice husk powder, and prolonging the washing time would increase the ignition

Table 10. Elemental Analysis for the Different Measuring Points of Rice Husk Ash by SEM (EDS) (70-18-K)

		mass fraction of main elements (%)							
	measuring point	C	Si	O	K	Fe	Ca	Mg	Mn
600 °C	1	10.83	34.46	46.82					
	2		28.18	45.63	1.02	15.21	1.07		
815 °C	1		54.22	38.21	0.89				
	2		48.20	40.8		1.96	1.67		
	3		46.93	42.28		1.93	2.28		
	4	38.18	38.04	18.87		1.72			
	5		43.54	48.26					
1100 °C	1		36.76	55.56					
	2		43.97	50.73					
	3		43.69	44.04		1.75	2.43		

https://doi.org/10.1021/acsomega.4c08820
ACS Omega 2024, 9, 50705−50719

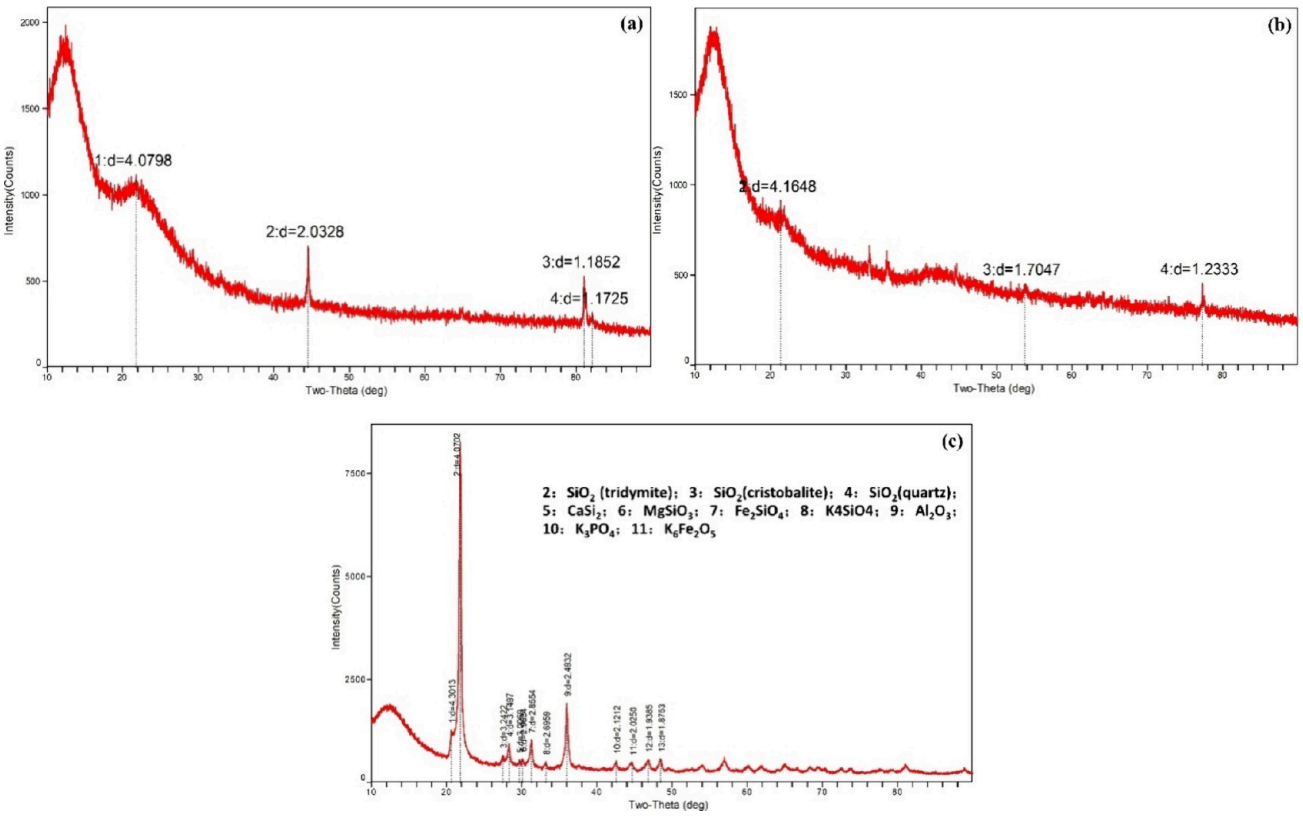

Figure 17. XRD spectrum of rice husk ash (70-18-K). (a) Sintering temperature of 600 °C, (b) sintering temperature of 815 °C, and (c) sintering temperature of 1100 °C.

temperature. Under the same washing conditions, the temperature of maximum rate of decomposition for rice husk powder and original rice husk could differ by 5−10 °C. For the original rice husk, the longer the washing time, the more unfavorable it was to increase the maximum weight loss rate. For rice husk powder, the effect was opposite. Therefore, the coupling effect of washing temperature and time on the combustion characteristics of rice husk was obvious. The coupling effect of particle size and washing time on the comprehensive characteristics of volatile release was obvious. Long-time washing was more beneficial to improve the combustion characteristics of rice husk and promote the increase in calorific value.

2. The flammability index C_r, burnout temperature T_f, and volatile devolatilization initial temperature T_s were sensitive to washing temperature. With the increase in washing temperature, the above three parameters increased obviously. The particle size d of washed rice husk was positively correlated with the volatile devolatilization initial temperature T_s, the temperature of maximum rate of decomposition T_{max}, and the burnout temperature T_f. The comprehensive characteristic index of volatile release D was negatively correlated with the particle size of washed rice husk. With increasing washing time, the smaller rice husk particle size presented a larger integrated combustion property index S, but the original rice husk presented better combustion characteristics with shorter washing time.
3. Washing original rice husk and rice husk powder could reduce the ash content to varying degrees, which was about 15% lower than that of rice husk without washing. In addition, because the surface structure of unmilled rice husk was more likely to adsorb ions and impurities, the alkali metals that have been dissolved in the washing solution would have an ion exchange effect with the rice husk. In the same washing time and temperature, the washing removal effect for alkali metal in rice husk powder was better than that in original rice husk, and the proportion of K in the ash sample decreases from 1 to 4% (washed rice husk) to 0.2−1%, and the ash deposit and slagging phenomenon of washed rice husk powder had been significantly improved. Under the same washing time, the higher the washing temperature was, the better the removal effect of alkali metals in washed rice husk was. Correspondingly, the proportion of high-temperature refractory Mg−Fe−Al acid salt increased in the high-temperature sintering stage, which effectively improved the ash melting point and reduced the probability of ash deposition and slagging.

AUTHOR INFORMATION

Corresponding Author

Shuo Yang − *Laboratory of Liaoning Province for Clean Combustion Power Generation and Heating Supply Technology, Shenyang Institute of Engineering, Shenyang 110136, China;* orcid.org/0000-0002-9404-3583; Email: ys_yang_shuo@163.com

Authors

Jintao Luo − *Laboratory of Liaoning Province for Clean Combustion Power Generation and Heating Supply Technology, Shenyang Institute of Engineering, Shenyang 110136, China*

https://doi.org/10.1021/acsomega.4c08820
ACS Omega 2024, 9, 50705−50719

Yu Gao − *Laboratory of Liaoning Province for Clean Combustion Power Generation and Heating Supply Technology, Shenyang Institute of Engineering, Shenyang 110136, China*
Shaohui Wang − *Laboratory of Liaoning Province for Clean Combustion Power Generation and Heating Supply Technology, Shenyang Institute of Engineering, Shenyang 110136, China*
Yupeng Zhang − *Laboratory of Liaoning Province for Clean Combustion Power Generation and Heating Supply Technology, Shenyang Institute of Engineering, Shenyang 110136, China*
Yuhang Wang − *Laboratory of Liaoning Province for Clean Combustion Power Generation and Heating Supply Technology, Shenyang Institute of Engineering, Shenyang 110136, China*
Pushi Ge − *Laboratory of Liaoning Province for Clean Combustion Power Generation and Heating Supply Technology, Shenyang Institute of Engineering, Shenyang 110136, China*
Wanqi Li − *Laboratory of Liaoning Province for Clean Combustion Power Generation and Heating Supply Technology, Shenyang Institute of Engineering, Shenyang 110136, China*
Yunyi Zheng − *Laboratory of Liaoning Province for Clean Combustion Power Generation and Heating Supply Technology, Shenyang Institute of Engineering, Shenyang 110136, China*
Jie Cui − *Laboratory of Liaoning Province for Clean Combustion Power Generation and Heating Supply Technology, Shenyang Institute of Engineering, Shenyang 110136, China*
Yudong Fu − *Laboratory of Liaoning Province for Clean Combustion Power Generation and Heating Supply Technology, Shenyang Institute of Engineering, Shenyang 110136, China*
Honggang Pan − *Laboratory of Liaoning Province for Clean Combustion Power Generation and Heating Supply Technology, Shenyang Institute of Engineering, Shenyang 110136, China*

Complete contact information is available at: https://pubs.acs.org/10.1021/acsomega.4c08820

Notes

The authors declare no competing financial interest.

■ ACKNOWLEDGMENTS

The present work is supported financially by the Science and Technology Joint Plan Project of Liaoning Province (2023JH2/101700256), Superior College Science and Technology Research Project of Liaoning Province (LJKZZ20220138), Basic Scientific Research Projects for Colleges and Universities under the Education Department of Liaoning Province (LJ242411632102 and 2023JH1/10400050).

■ REFERENCES

(1) Bazargan, A.; Bazargan, M.; McKay, G. Optimization of rice husk pretreatment for energy production. *Renew. Energy* **2015**, *77*, 512−520.
(2) Tayeh, B. A.; Alyousef, R.; Alabduljabbar, H.; Alaskar, A. Recycling of rice husk waste for a sustainable concrete: a critical review. *J. Clean. Prod.* **2021**, *312*, No. 127734.
(3) Quispe, I.; Navia, R.; Kahhat, R. Energy potential from rice husk through direct combustion and fast pyrolysis: a review. *Waste manage.* **2017**, *59*, 200−210.
(4) Cuong, T. T.; Le, H. A.; Khai, N. M.; Hung, P. A.; Linh, L. T.; Thanh, N. V.; Tri, N. D.; Huan, N. X. Renewable energy from biomass surplus resource: potential of power generation from rice straw in Vietnam. *Sci. Rep-uk.* **2021**, *11* (1), 792.
(5) Wu, J.; Yu, D.; Zeng, X.; Yu, X.; Han, J.; Wen, C.; Yu, G. Ash formation and fouling during combustion of rice husk and its blends with a high alkali Xinjiang coal. *Energy Fuels* **2018**, *32* (1), 416−424.
(6) Ahiduzzaman, M.; Sadrul Islam, A. K. M. Preparation of porous bio-char and activated carbon from rice husk by leaching ash and chemical activation. *SpringerPlus* **2016**, *5* (1), 1248.
(7) Linam, F.; Limmer, M. A.; Ebling, A. M.; Seyfferth, A. L. Rice husk and husk biochar soil amendments store soil carbon while water management controls dissolved organic matter chemistry in well-weathered soil. *J. Environ. Manage.* **2023**, *339*, No. 117936.
(8) Rendón, J.; Giraldo, C. H. C.; Monyake, K. C.; Alagha, L.; Colorado, H. A. Experimental investigation on composites incorporating rice husk nanoparticles for environmental noise management. *J. Environ. Manage.* **2023**, *325*, No. 116477.
(9) Kordi, M.; Farrokhi, N.; Pech-Canul, M. I.; Ahmadikhah, A. Rice husk at a glance: from agro-industrial to modern applications. *Rice Sci.* **2024**, *31* (1), 14−32.
(10) Carmona, V. B.; Oliveira, R. M.; Silva, W. T. L.; Mattoso, L.; Marconcini, J. Nanosilica from rice husk: extraction and characterization. *Ind. Crop. Prod.* **2013**, *43*, 291−296.
(11) Le, Q. T. N.; Hwang, I. Stabilization of hydrophobic organic compounds in sediment using alkali-activated rice husk biochar: Enhancement of sorption by dissolved organic matter. *Chem. Eng. J.* **2023**, *476*, No. 146513.
(12) Niu, Y.; Lv, Y.; Lei, Y.; Liu, S.; Liang, Y.; Wang, D.; Hui, S. Biomass torrefaction: properties, applications, challenges, and economy. *Renew. Sust. Energy Rev.* **2019**, *115*, No. 109395.
(13) Guo, X.; Yang, X.; Shang, Y.; Lv, Y.; Niu, Y. Solidification and leaching behaviours of heavy metal Pb in MSW incineration fly ash and its thermal stability at various thermal treatment temperatures. *Fuel* **2024**, *372*, No. 132130.
(14) Ma, Y.; Zhang, H.; Yang, H.; Zhang, Y. The effect of acid washing pretreatment on bio-oil production in fast pyrolysis of rice husk. *Cellulose* **2019**, *26*, 8465−8474.
(15) Hiremath, P. G.; Chennabasappa, M.; C, M.; V, T. Fluoride removal using tartaric acid-modified rice husk biochar: Comprehensive batch and column studies. *Sustainable Chem. One World* **2024**, *2*, No. 100005.
(16) Fang, Q.; Ji, S.; Huang, D.; Huang, Z.; Huang, Z.; Zeng, Y.; Liu, Y. Impact of alkaline pretreatment to enhance volatile fatty acids (VFAs) production from rice husk. *Biochem. Res. Int.* **2019**, *2019* (1), 1.
(17) Pinto, F.; Gominho, J.; André, R. N.; Gonçalves, D.; Miranda, M.; Varela, F.; Neves, D.; Santos, J.; Lourenço, A.; Pereira, H. Effect of rice husk torrefaction on syngas production and quality. *Energy Fuels* **2017**, *31* (5), 5183−5192.
(18) Hafid, H. S.; Omar, F. N.; Zhu, J.; Wakisaka, M. Enhanced crystallinity and thermal properties of cellulose from rice husk using acid hydrolysis treatment. *Carbohyd polym.* **2021**, *260*, No. 117789.
(19) Ninduangdee, P.; Kuprianov, V. I. Fluidized bed co-combustion of rice husk pellets and moisturized rice husk: The effects of co-combustion methods on gaseous emissions. *Biomass Bioenerg.* **2018**, *112*, 73−84.
(20) Yang, C.; Fang, T. Kinetics for enzymatic hydrolysis of rice hulls by the ultrasonic pretreatment with a bio-based basic ionic liquid. *Biochem. Eng. J.* **2015**, *100*, 23−29.
(21) Saba, M.; Khan, A.; Ali, H.; Bibi, A.; Gul, Z.; Khan, A.; Rehman, M. M. U.; Badshah, M.; Hasan, F.; Shah, A. A.; Khan, S. Microbial pretreatment of chicken feather and its co-digestion with rice husk and green grocery waste for enhanced biogas production. *Front. Microbiol.* **2022**, *13*, No. 792426.

(22) Wang, Y.; Li, B.; Gao, A.; Ding, K.; Xing, X.; Wei, J.; Huang, Y.; Chun-Ho Lam, J.; Subramanian, K. A.; Zhang, S. Volatile-char interactions during biomass pyrolysis: Effect of biomass acid-washing pretreatment. *Fuel.* **2023**, *340*, No. 127496.
(23) Kim, J. S.; Lee, Y. Y.; Kim, T. H. A review on alkaline pretreatment technology for bioconversion of lignocellulosic biomass. *Bioresource technol.* **2016**, *199*, 42−48.
(24) Zhang, S.; Su, Y.; Xu, D.; Zhu, S.; Zhang, H.; Liu, X. Assessment of hydrothermal carbonization and coupling washing with torrefaction of bamboo sawdust for biofuels production. *Bioresource technol.* **2018**, *258*, 111−118.
(25) Bussemaker, M. J.; Zhang, D. Effect of ultrasound on lignocellulosic biomass as a pretreatment for biorefinery and biofuel applications. *Ind. Eng. Chem. Res.* **2013**, *52* (10), 3563−3580.
(26) Carrillo, M. A.; Staggenborg, S. A.; Pineda, J. A. Washing sorghum biomass with water to improve its quality for combustion. *Fuel* **2014**, *116*, 427−431.
(27) Hensgen, F.; Wachendorf, M. Aqueous leaching prior to dewatering improves the quality of solid fuels from grasslands. *Energies* **2018**, *11* (4), 846.
(28) Gudka, B.; Jones, J. M.; Lea-Langton, A. R.; Williams, A.; Saddawi, A. A review of the mitigation of deposition and emission problems during biomass combustion through washing pre-treatment. *J. Energy Inst.* **2016**, *89* (2), 159−171.
(29) Deng, L.; Zhang, T.; Che, D. Effect of water washing on fuel properties, pyrolysis and combustion characteristics, and ash fusibility of biomass. *Fuel Process. Technol.* **2013**, *106*, 712−720.
(30) Ma, Q.; Han, L.; Huang, G. Evaluation of different water-washing treatments effects on wheat straw combustion properties. *Bioresource technol.* **2017**, *245*, 1075−1083.
(31) Hedman, B.; Boström, D.; Zhu, W.; Örberg, H.; Xiong, S. Enhancing fuel qualities of cassava crop residues by washing. *Fuel Process. Technol.* **2015**, *139*, 127−134.
(32) Zhao, X.; Yang, F.; Tan, H.; Jiao, Y.; Zhou, M. Effect of the water washing pretreatment on biomass pyrolysis in CO_2 atmosphere. *J. Energy. Inst.* **2024**, *115*, No. 101697.
(33) Tan, C.; Saritpongteeraka, K.; Kungsanant, S.; Charnnok, B.; Chaiprapat, S. Low temperature hydrothermal treatment of palm fiber fuel for simultaneous potassium removal, enhanced oil recovery and biogas production. *Fuel* **2018**, *234*, 1055−1063.
(34) Singhal, A.; Konttinen, J.; Joronen, T. Effect of different washing parameters on the fuel properties and elemental composition of wheat straw in water-washing pre-treatment. Part 1: Effect of washing duration and biomass size. *Fuel* **2021**, *292*, No. 120206.
(35) Singhal, A.; Konttinen, J.; Joronen, T. Effect of different washing parameters on the fuel properties and elemental composition of wheat straw in water-washing pre-treatment. Part 2: Effect of washing temperature and solid-to-liquid ratio. *Fuel* **2021**, *292*, No. 120209.
(36) Iáñez-Rodríguez, I.; Martín-Lara, M. Á.; Pérez, A.; Blázquez, G.; Calero, M. Water washing for upgrading fuel properties of greenhouse crop residue from pepper. *Renew. Energy* **2020**, *145*, 2121−2129.
(37) Liu, L.; Pang, Y.; Lv, D.; Wang, K.; Wang, Y. Thermal and kinetic analyzing of pyrolysis and combustion of self-heating biomass particles. *Process Saf. Environ.* **2021**, *151*, 39−50.
(38) Xiang, Y.; Xiang, Y.; Wang, L. Thermal decomposition kinetic of hybrid poplar sawdust as biomass to biofuel. *J. Environ. Chen. Eng.* **2016**, *4* (3), 3303−3308.
(39) Zhang, W.; Jia, J.; Zhang, J.; Ding, Y.; Zhang, J.; Lu, K.; Mao, S. Pyrolysis and combustion characteristics of typical waste thermal insulation materials. *Sci. Total Environ.* **2022**, *834*, No. 155484.
(40) Wang, C.; Bi, H.; Lin, Q.; Jiang, X.; Jiang, C. Co-pyrolysis of sewage sludge and rice husk by TG−FTIR−MS: Pyrolysis behavior, kinetics, and condensable/non-condensable gases characteristics. *Renew. Energy* **2020**, *160*, 1048−1066.
(41) Chen, G.; Li, J.; Lin, H.; Wu, F.; Chao, Y. A study of the production and combustion characteristics of pyrolytic oil from sewage sludge using the taguchi method. *Energies* **2018**, *11* (9), 2260.
(42) Han, K.; Wang, Q.; Zhao, J.; Luo, K.; Li, H.; Chen, Y.; Lu, C. Combustion pattern, characteristics, and kinetics of biomass and chars from segmented heating carbonization. *Asia-Pac. J. Chen. Eng.* **2016**, *11* (5), 812−822.
(43) Cheng, J.; Sun, X. Determination of the devolatilization index and combustion characteristic index of pulverized coals. *Power Eng.* **1987**, *7* (5), 33−6.
(44) He, D.; Saito, K.; Kato, T.; Kosugi, C.; Shimohara, T.; Nakabayashi, K.; Yoon, S.-H.; Miyawaki, J. Unveiling the hidden intrinsic porosity of marine biomass-derived carbon: Eliminating pore-blocking minerals. *Carbon* **2024**, *3* (1), 18−28.
(45) Wang, Q.; Wang, G.; Zhang, J.; Lee, J.-Y.; Wang, H.; Wang, C. Combustion behaviors and kinetics analysis of coal, biomass and plastic. *Thermochim. Acta* **2018**, *669*, 140−148.
(46) Hsuan, C.; Hou, S. Co-combustion characteristics and kinetics of sludge/coal blends in 21%−50% oxygen-enriched O_2/CO_2 atmospheres. *Fuel* **2024**, *362*, No. 130821.
(47) White, J.; Catallo, W.; Legendre, B. Biomass pyrolysis kinetics: a comparative critical review with relevant agricultural residue case studies. *J. Anal. Appl. Pyrol.* **2011**, *91* (1), 1−33.

https://doi.org/10.1021/acsomega.4c08820
ACS Omega 2024, 9, 50705−50719